GROUND MOTIONS FROM LARGE EARTHQUAKES (MW³7) ON THE SANTA MONICA MOUNTAIN THRUST AND HOLLYWOOD-SANTA MONICA-MALIBU FAULTS

C K SAIKIA[1] And P G SOMMERVILLE[2]

SUMMARY

We have simulated ground motion parameters for engineering use at eighteen urban centers located along the Santa Monica Mountain fault system for earthquakes occurring on the Hollywood-Santa Monica-Malibu (HF-SMF-MF) and Santa Monic Mountain Thrust (SMMTF) faults. These urban centers, which include Beverly Hills, Westwood, Sherman Oaks, Santa Monica, Century City, and downtown Los Angeles, have many multi-story buildings. Of these, thirteen have CSMIP strong motion instruments which recorded the 1994 Northridge earthquake. In this study, we considered three earthquake scenarios: a M_w 7 earthquake on the HF-SMF-MF fault which has a dip of 70^o and a strike of 255.8^o for the HF, 239.8^o for the SMF and 270^o for the MF, and a rake of 5^o; a M_w 7 earthquake on the buried SMMTF which has a dip of 20^o, a strike of 258.5^o and rake of 90^o , and a M_w 7.2 earthquake which is generated by a simultaneous rupturing of these two faults. To produce ground motion parameter for the simultaneous rupture, broadband time histories simulated for the two fault systems were added with appropriate time lags. Each M_w 7 earthquake was simulated using a fault surface with a length of 52 km and a width of 18 km. Broadband time histories were simulated using 9 hypocenters and 10 randomly generated slip models. Thus for each site, we simulated a total of 180 horizontal component ground motion time histories for each earthquake scenario. To further investigate the influence of basin structure on levels of ground motions at each site, we conducted two separate simulations; one with a common 1D structure for all sites which has a surface shear-wave velocity of 1 km/sec and the other with site-specific velocity structure extracted from the updated 3D velocity structure of the Los Angeles basin (SCEC, 1998). In these site-specific models the surface shear-wave velocity are as low as 0.5 km/sec. Based on this simulation study, we conclude that the peak ground accelerations from the Hollywood fault dominate the ground motions from the Santa Monica Mountain thrust fault system. In general, peak ground accelerations from the Hollywood fault earthquake are 2 to 2.5 times larger than the peak ground accelerations from the Santa Monica Mountain thrust fault at sites *hsbg, shro, nhol, lacc, smn, bvh, ulg, la19*, and *ul7*. These large motions are primarily caused by the shallow depth and proximity of the Hollywood-Santa Monica fault to the selected sites. This shallow depth of the Hollywood-Santa Monica fault system also contributes significantly to the long-period ground motions. Results of this simulation study are briefly summarized in this study.

INTRODUCTION

Ground motions observed during the 1994 Northridge earthquake demonstrated that empirical attenuation relations may not sometimes provide accurate estimates of ground motions from an earthquake occurring on a known or previously unidentified fault without any episode of previous large earthquakes. One lesson from this earthquake was that a moderate sized earthquake in the greater Los Angeles region can produce damage and loss of life much greater than that due to the earthquakes on the San Andreas fault. Illustrations of such severe damage from past large earthquakes in the Los Angeles region include the 1933 Long Beach (M»6.3), the 1971

[1] *URS Greiner Woodward Clyde, 566 El Dorado Street, Pasadena, CA, USA email: chandan_saikia@urscorp.com*
[2] *URS Greiner Woodward Clyde, 566 El Dorado Street, Pasadena, CA, USA*

San Fernando (M»6.7) and the 1987 Whittier (M» 5.9) earthquakes. There are other faults in the region which are capable of generating moderate to large earthquakes which may incur significant loss and damage to vulnerable buildings and bridges in the nearby urban centers located adjacent to these faults. To mitigate seismic losses in the event of large earthquakes, it is possible to retrofit such vulnerable buildings and bridges, and construct new infrastructure provided reliable design spectra representing the source and propagation related seismic effects from the probable damaging earthquakes are available.

The use of empirical design spectra that are processed and scaled from recordings of large earthquakes is widespread in the engineering community. The various drawbacks with this approach are that the chosen empirical design spectra may not relate to the physical process of the earthquakes controlling the seismic hazard and may not have the extended duration and amplification of ground motions in complex regions like within the Los Angeles basin. They may also lack the near-source velocity pulse caused by the rupture directivity. These drawbacks can be overcome using time histories simulated based on modern seismological methods with appropriate crustal models and fault geometry.

The Santa Monica Mountain fault zone (SMMFZ) is capable of producing large earthquakes (Dolan *et al.*, 1995; WCGEP, 1995). The Santa Monica Mountains thrust (SMMT) ramp which is capable of producing earthquakes as large as M_w 7.3 (Dolan *et al.*, 1995), is a blind thrust and is a member of the provisional segmentation model (WCGEP, 1995). A co-rupture of the Santa Monica Mountain thrust fault (SMMTF) and the Hollywood thrust-Santa Monica Fault-and Malibu strike-slip fault (HF-SNF-MF) can produce an earthquake even of larger magnitude. The estimate of large magnitude for these earthquakes is based on a seismic-moment deficit hypothesis suggested by Dolan *et al.* (1995). In recent studies Stein and Hanks (1998) concluded that there is no deficit in the release of seismic moment in southern California catalog for earthquakes of M³6, no increase in the rate of M³6 earthquakes, and finally no evidence for huge but rare earthquakes in the region. Even though these observations can alter views on the earthquake hazards and risk assessment in southern California, they do not alter by any means the fact that large earthquakes are likely to occur on faults that have not ruptured in recent times in southern California. The SMMFZ falls into this category and is located adjacent to the major urban centers containing buildings that are 3 to 20 stories tall. Faults are large in dimensions and are capable of producing large earthquakes. The rupture directivity alone can produce large velocity pulses, thus raising safety issue to the tall buildings that lie along this entire fault zone.

For earthquakes likely to occur on the HF-SMF-MF and SMMTF faults, we generated and analyzed time histories at 18 sites located adjacent to the SMMFZ (Figure 1). The thick solid line is the map view of the actual fault (Wright, 1991). The other three thin lines represent the segments that were used in the actual simulation study. The sites have varying local conditions. For example, sites *hsbg* and *la19* are underlain by deep alluvium, sites *lacc, ulg, la12, la9,* and *ul7* by alluvium, site *la15* by sedimentary rock, and sites *la13* and *la52* by alluvium over the sedimentary rock materials (Table 1). These effects were also included in our time histories. While the HF-SMF-MF fault is tractable, the SMMTF is buried which we assumed to be buried at a depth of 14.23 km. The simulated time histories and spectral values were analyzed to determine which of the sites are exposed to significant ground motions, which fault dominates ground motions, whether the empirical ground motions estimated from the attenuation relation (Abrahamson and Silva, 1997) are adequate, and how the 1D approache at best can represent the basin effect.

SIMULATION PROCEDURE

The technique used for simulation is similar to the method used to generate broadband ground motion time histories in our earlier works (Somerville et al., 1995 and Saikia and Somerville, 1997). Our earlier method was further modified to include the ability for simulating ground motions for a multi-segmented fault. For a fault having segments striking at different azimuths, time histories are simulated for each segment separately. Using the same width and length of the entire fault for each segment, seismic moment distribution on the fault surface is set to zero for the portions belonging to the other segments. The weights of individual elements are normalized by the total weights on the entire fault, so that the seismic moment partition is correct. The fault is allowed to have the strike and dip of the segment for which simulation is needed. Hence, the site co-ordinates keep varying from one segment simulation to the other. The time histories for the the segments are then added to generate time histories for the entire fault. This scheme of mutiple-segment simulation was calibrated by conducting a simulation for a fault in which all segments were given the same dip and strike and by comparing the time histories with those of a single simulation for the entire fault. We applied this method to simulate time histories for the Hollywood Santa Monica fault whose various segments have different strikes as stated in the

abstract. The Santa Monica thrust fault was simulated as a single fault. Its location and burial depth have not yet been well-established and our values are only approximate.

ASPERITY MODELS

Each M_w 7 earthquake was simulated using a fault surface having a length of 52 km and width of 18 km. Time histories were generated for 9 hypocenters and 10 randomly generated slip models using the algorithm discussed in Saikia and Somerville (1997). Many slip models were generated and those capturing variations in the locations of asperities on the fault surface were selected to ensure that the average ground motion parameters estimated from the simulation are least biased towards a particular asperity distribution. In regards to the depth of burial of the Hollywood Santa Monica fault, we analyzed distrbution of seismicity adjacent to the fault (Figure 1) and found evidence of the shalllow seismic activity. So, it was buried at a depth of 0.4 km.

CRUSTAL WAVEGUIDE

Several crustal structures were used to generate time histories. The first model was derived by combining the southern California model and the shallow Los Angeles basin model. It consisted of 8 layers of which the top 5 layers have a total thickness of 7 km representing the deepest part of the LA basin structure. This model may not be the appropriate as the SMMFZ is away from the deeper part of the LA basin. But we continued with this model as several sites are located in Los Angeles downtown. In this model, the minimum shear-wave velocity at the surface is prescribed at 1 km/s. In addition, we also extracted one-dimensional velocity structures for each site from the three-dimensional LA basin model which was recently released by the Southern California Earthquake Center (SCEC). Figure 2 shows these various crustal models. These models have the surface shear-wave velocity ranging from about 0.1km/s to 0.3 km/s. Assuming a surface shear-wave velocity of 0.5 km/s, the sites seem to fall in three categories based on the depth dependence up to a velocity of 1 km/s. The thick lines show the average representations of these three categories. The category-I represents the Santa Monica (smn) site. The category-II represents three sites, namely *lacc, la19* and *bvh;* and the category-III includes *shro, hsbg, ulg, ul7, la9, la12, la13, la15, la52, la54 a*nd *ulH.* The other two sites, *nhol and glen* have the surface shear-wave velocity same as that of the average 1D model developed for all sites.

RESULTS

For each site, we had simulated a total of 180 horizontal components of ground motion time histories for 10 slip models separately for the average 1D crustal model and for the other models to include site effects. This was done for both the Santa Monica thrust and HF-SMF-MF faults. These time histories were used to computed average peak ground accelerations and 84^{th} percentile at each site and evaluate the amplification level that was caused just by the impedance contrast between the 1D and 3D models. Our model based simulations do not account for the effects of irregular basin boundaries, especially the effects noted at the basin edge near Santa Monica during the 1994 Northridge earthquake (Hartzell *et al.*, 1997; Graves *et al.*, 1998). These effects may not also be observed from the earthquakes that we are studying as the sites are located adjacent to the fault. The basin edge structure that is present near Santa Monica (Wright, 1991) is normal to the path from the Northridge earthquake. For this earthquake, the path provided a waveguide for the diffracted surfaces wave to interfere with the direct S waves. In the present simulation, only segment that may induce significant basin effects is probably the EW trending segment located west of Santa Monica.

This study showed that the peak ground accelerations from the Hollywood fault dominate the ground motions from the Santa Monica thrust fault. In general, they are 2 to 2.5 times larger at sites *hsbg, shro, nhol, lacc, smn, bvh, ulg, la19*, and *ul7.* These ground motions are caused primarily by the shallow depth and proximity of the Hollywood-Santa Monica fault to the selected sites. At sites, *la52, la54, la15. la13, la12* and *la9* which are located in Los Angeles downtown, accelerations from the Holllywood-Santa Monica fault are larger by a factor about 2. All time histories were processed to analyze the spectral values for each scenario. Spectral values were averaged over all the hypocenters and slip models. For the values estimated from the rock model i.e., the average 1D model for the rock-site structure, they are compared with the estimates from the empirical attenuation relation of Abrahamson and Silva (1997) for rock. The median spectral values lie above the

empirical median values, especially for the shallow Hollywood-Santa Monica fault, but lie within one standard deviation from the mean of these empirical estimates at most of the sites. The empirical ground motions estimated for the Santa Monica thrust fault are consistent with those simulated in this study. This is also noted in an on-going study in which the estimated ground motions from the empirical relation are compared with the recorded ground motions of individual earthquakes which are either buried or have surface rupture. At several sites, for example *hsbg, shro, nhol, lacc, bvh, gle, ulg,* and *ul7,* the long-period (1-3s) spectral values are significantly higher than those predicted using the empirical relation. In particular, hypocenters located at the western edge of the fault cause the simulated median motion to become large due to the rupture directivity effect.

To include the site conditions ranging from category I to III, time histories were simulated at 15 sites. Figure 3 shows a set of time histories simulated at site *smn* for the two earthquake scenarios and varying site conditions for 9 hypocenters for one slip model. The upper two panels show time histories for the Hollywood Santa Monica fault and the bottom two panels show for the Santa Monica thrust fault. The panels on right show accelerograms simulated specific to the category-I site conditions. Clearly, the level of ground motion amplification is different depending upon the locations of the hypocenter. Also, the time histories from the Hollywood Santa Monica fault is dominated by a strong single pulse for all hypocentral locations. To account for site effects, we processed the time histories and measured two ratios of spectral accelerations and velocities for each site, one by measuring the ratios relative to the spectral value estimated for the rock structure (1 km/s) at the site and other by measuring the ratios relative to the spectral value estimated at three sites: *nhol, glen*, and *shro,* considered as the neighboring rock sites. The results are summarized in Figure 4. For each panel, the three columns from the left show spectral ratios measured from the simulation results corresponding to the Hollywood Santa Monica, Santa Monica thrust, and a simultaneous rupture of the two faults. Ground motions simulated for the Hollywood Santa Monica fault exhibit a major amplification, especially at long periods (> 1s). We are currently analyzing these results to identify the cause of this amplification.

REFERENCE

Abrahamson, N. and Silva, W. J. (1997). Empirical response spectra attenuation relations for shallow crustal earthquakes, *Seis. Res. Lett.*, 68, 94-127.

Dolan, J. F., Siek, K., Rockwell, T. K., Yeats, R. S., Shaw, J., Suppe, J., Huftile, G. J., and Gath, E. M. (1995). Prospects for larger or more frequent earthquakes in Los Angeles Metropolitan region, *Science*, 267, 199-205.

Graves, R. W., Pitarka, A., and Somerville, P. G. (1998). Ground-motion amplification in the Santa Monica area: effects of shallow basin-edge structure, *Bull. Seis. Soc. Am.*, 88, 1224-1242.

Hartzell, S., Cranswick, E., Frankel, A., Carver, D., and Meremonte M. (1997) Variability of site response in the Los Angeles urban area, *Bull. Seis. Soc. Am.*, 87, 1377-1400.

Saikia, C. K. and Somerville, P. G. (1997). Simulated hard-rock motions in Saint Louis, Missouri, from large New Madrid earthquakes, *Bull. Seis. Soc. Am.*, 87, 123-139.

Somerville, P. G., Graves, R. W., and C. K. Saikia (1995). *Characterization of ground motions at the sites of subject buildings*, Report on Task 4 of SAC Joint Venture Program for Reduction of Earthquake Hazards in Steel Moment Frame.

Stein, R. S. and Hanks, T. C. (1998). M³6 earthquakes in Souhthern California during the twentieth century: no evidence for a seismicity or moment deficit, *Bull. Seis. Soc. Am.*, 88, 635-652.

WGCEP (1995). Working group on California earthquake probabilities, seismic hazards in southern California: probable earthquakes, 1994-2014, *Bull. Seis. Soc. Am.*, 89. 379-439.

Wright, T. L. (1991). Structural geology and tectonic evolution of the Los Angeles basin, California, in Active Margin Basins: *AAPG Memoir 52*, K. E. Biddle (Editor), 35-134.

Table 1. Site Co-ordinates and Geology

Site	Latitude °N	Longitude °W	CSMIP code	Site Geology	Station Name
hsbg	34.09	118.339	24303	Deep Alluvium	LA, Hollywood Storage Bldg.
shro	34.154	118.465			Sherman, Thousand Oaks
nhol	34.138	118.359			North Hollwood
lacc	34.063	118.416	24390	Alluvium	Century City, Los Angeles
smn	34.0147	118.485			Santa Monica
bvh	34.068	118.401			Beverly Hills
glen	34.137	118.2455			Glendale
ulg	34.068	118.439	24688	Alluvium	LA, UCLA Grounds
la19	34.059	118.416	24643	Deep Alluvium	LA, 19-Story Office Bldg.
la52	34.051	118.259	24602	Alluvium over Sed. Rock	LA, 52-Story Office Bldg.
la54	34.048	118.260	24629	,,	LA, 54-Story Office Bldg.
la15	34.058	118.249	24569	Sedimentary Rock	LA, 15-Story Govern. Office Bldg.
la13	34.050	118.247	24567	Alluvium over Sed. Rock	LA, 13-Story Office Bldg.
la12	34.048	118.260	24581	Alluvium	LA, 12-Story Comm./Office Bldg.
la9	34.044	118.261	24579	Alluvium	LA, 9-Story Office Bldg.
ul7	34.069	118.442	24231	Alluvium	LA, 7-Story UCLA Math-Sci. Bldg.
ulH	34.062	118.198	24605	Silstone	LA, Univ. Hospital Grounds
ul8	34.067	-118.168	24468	Sedimentary Rock	LA, 8-Story CSULA Admin Bldg.

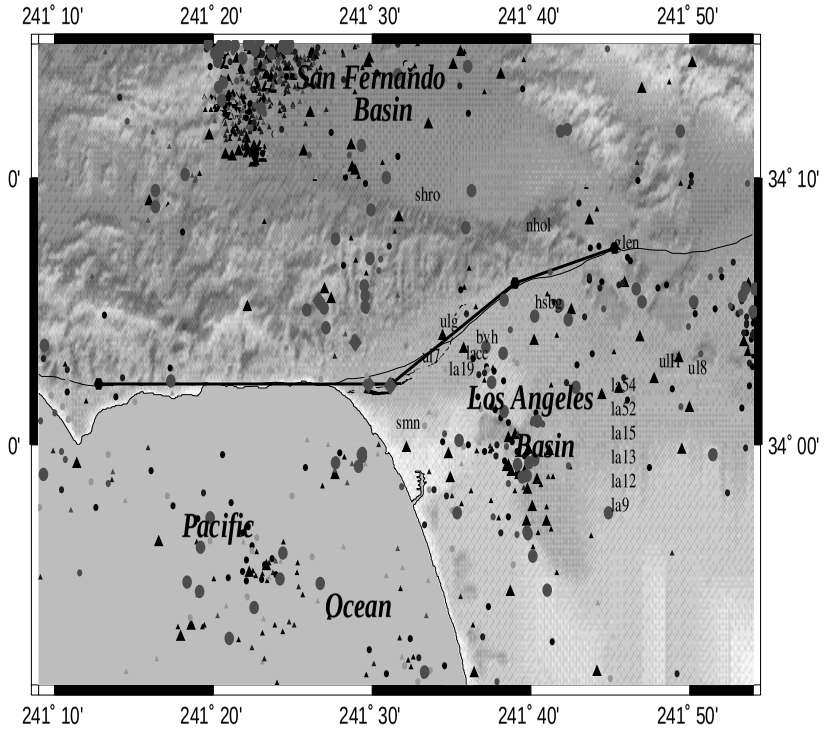

Figure 1. Map showing the locations of 18 sites and the orientation of the Hollywood Santa Monica fault. The thin lines show the projection of the fault on the surface (Wright, 1991) and thick three lines show the segments of the faults used in this study to simulate time histories. Also projected on this map is the distribution of seismicity around the fault; different symbols indicate magnitude and depth. The main conclusion of this seismicity distribution is that earthquakes are present up to shallow depth of 1 km in the proximity of the fault and so this fault was allowed to rupture to a depth of 0.4 km.

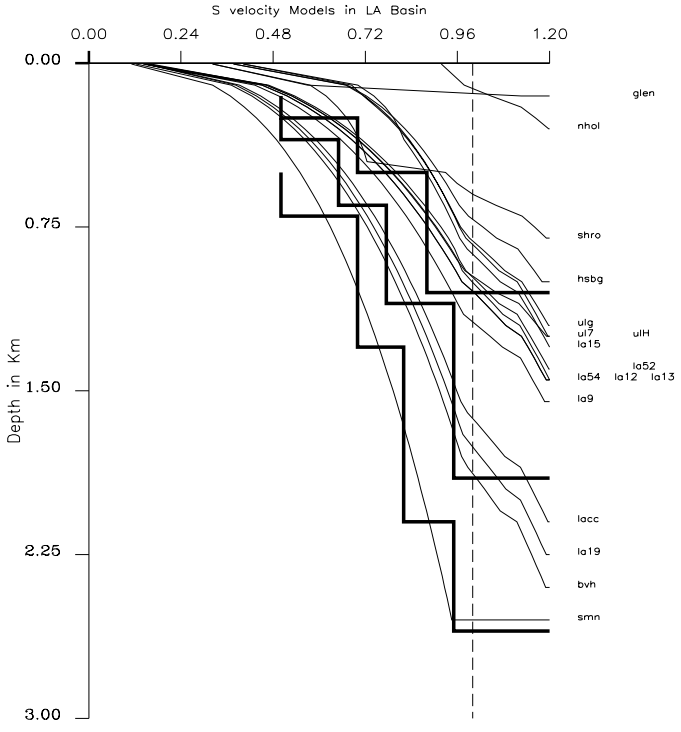

Figure 2. Thin lines represent 1D shows the distribution of S-wave velocities beneath each stations (station name is marked to the right of model line). This model distribution is extracted from the 3D model recently made available by SCEC. The thick solid lines show the average model representing a group of stations.

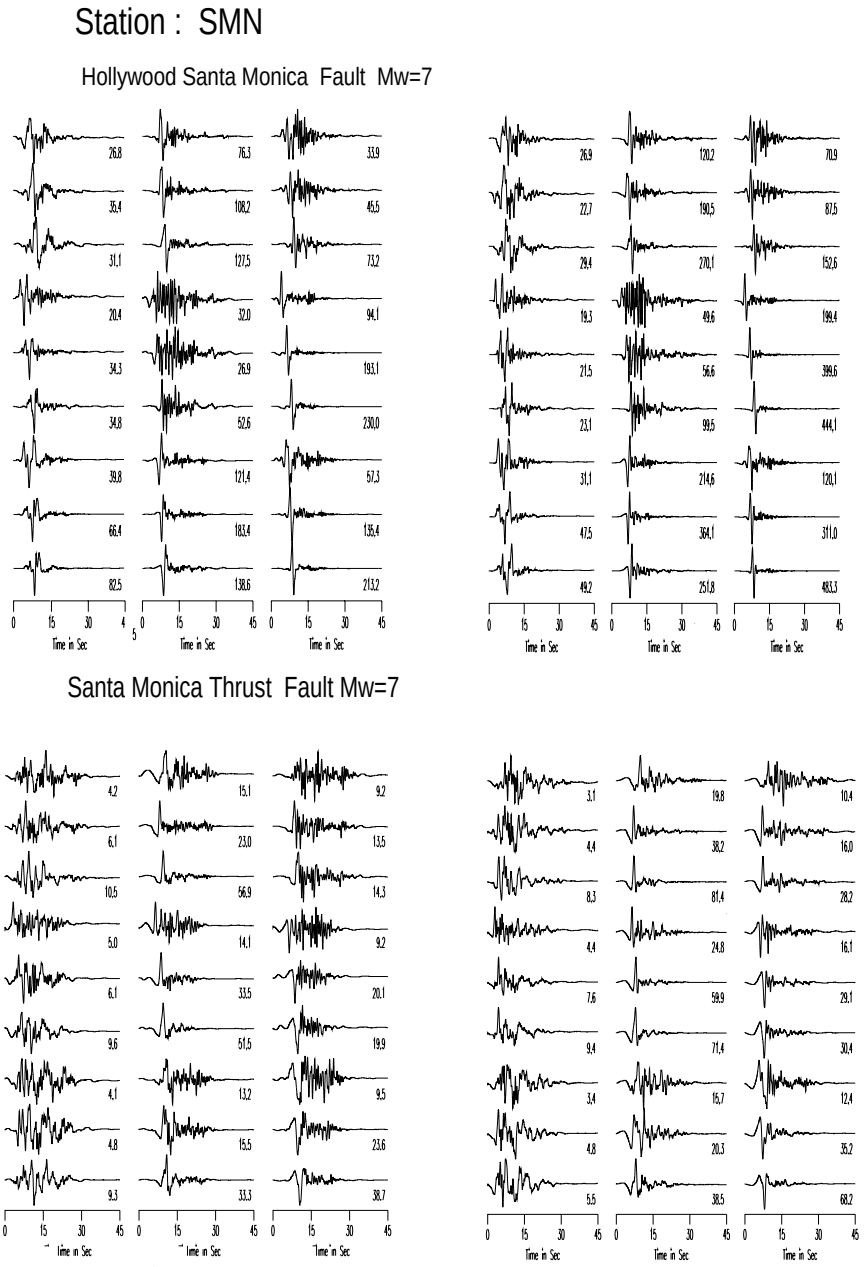

Figure 3. Example of time histories simulated for the Hollywood Santa Monica (top) and Santa Monica thrust (bottom) faults for 9 hypocenters for one slip model. In each panel, three accelerograms in a row correspond to the vertical and two horizontal components for one hypocenter. Panels on the left show time histories for rock-like structure with surface shear-wave velocity of 1 km/.s and on the right show corresponding simulation for the site category-I (smn) for which the surface shear-wave velocity is 0.5 km/sec. Note the amplification caused just by the local site model.

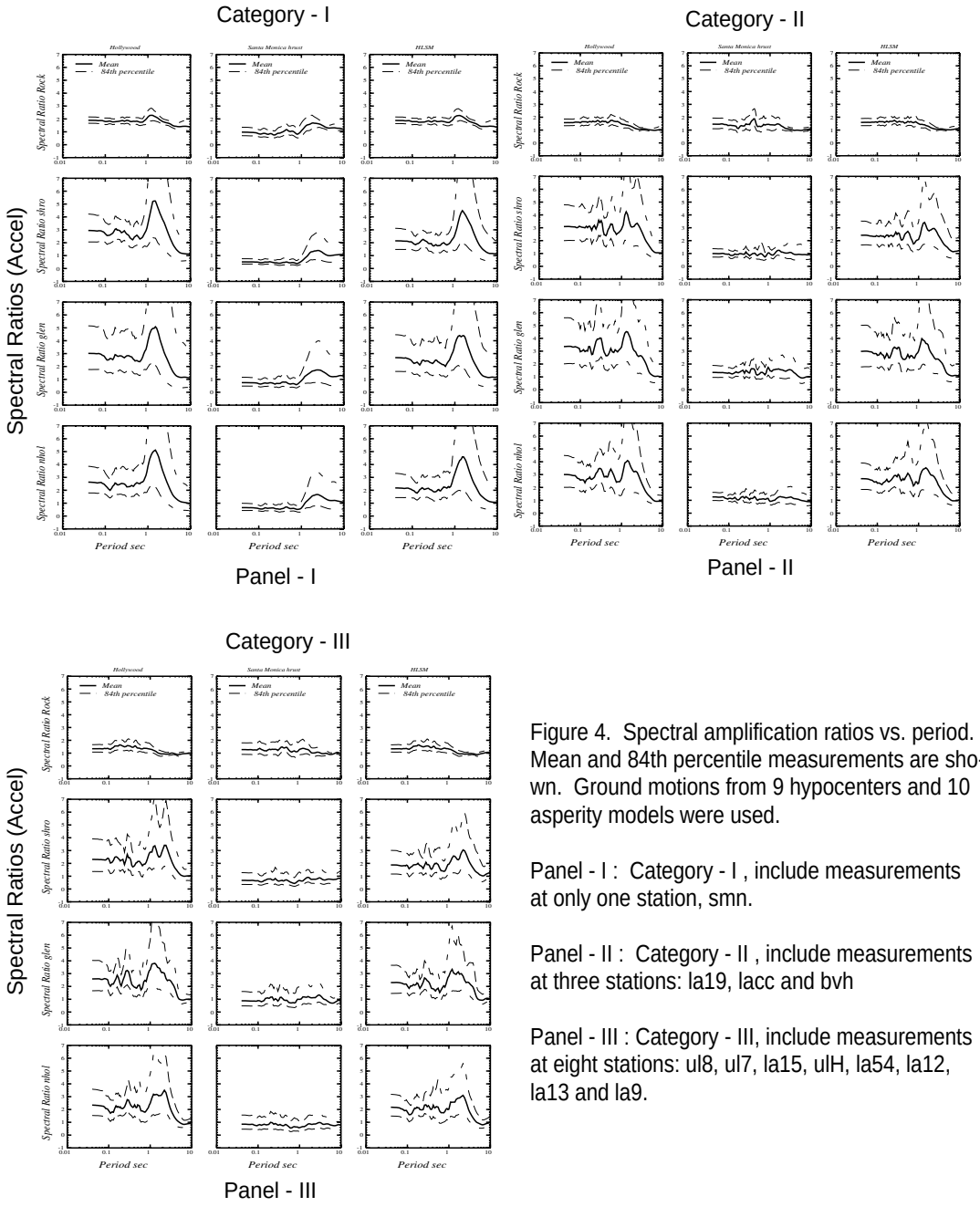

Figure 4. Spectral amplification ratios vs. period. Mean and 84th percentile measurements are shown. Ground motions from 9 hypocenters and 10 asperity models were used.

Panel - I : Category - I , include measurements at only one station, smn.

Panel - II : Category - II , include measurements at three stations: la19, lacc and bvh

Panel - III : Category - III, include measurements at eight stations: ul8, ul7, la15, ulH, la54, la12, la13 and la9.